THE GEOLOGICAL SOCIETY OF AMERICA®

Paradigm shift in determining Neoproterozoic atmospheric oxygen

Nigel J.F. Blamey[1,2,3], Uwe Brand[1], John Parnell[3], Natalie Spear[4], Christophe Lécuyer[5], Kathleen Benison[6], Fanwei Meng[7], and Pei Ni[8]

[1]Department of Earth Sciences, Brock University, 1812 Sir Isaac Brock Way, St Catharines, Ontario L2S 3A1, Canada
[2]Department of Earth and Environmental Science, New Mexico Tech, 801 Leroy Place, Socorro, New Mexico 87801, USA
[3]Department of Geology and Petroleum Geology, University of Aberdeen, AB24 3Ue Aberdeen, Scotland
[4]Department of Earth and Environmental Science, University of Pennsylvania, Philadelphia, Pennsylvania 19014, USA
[5]Laboratoire de Géologie de Lyon, UMR CNRS 5276, University of Lyon and Institut Universitaire de France, 69622 Villeurbanne, France
[6]Department of Geology and Geography, University West Virginia, Morgantown, West Virginia 26506, USA
[7]Nanjing Institute of Geology and Palaeontology, Chinese Academy of Sciences, #39 East Beijing Road, Nanjing 210008, China
[8]School of Earth Sciences and Engineering, Nanjing University, Nanjing 210093, China

ABSTRACT

We present a new and innovative way of determining the oxygen level of Earth's past atmosphere by directly measuring inclusion gases trapped in halite. After intensive screening using multiple depositional, textural/fabric, and geochemical parameters, we determined that tectonically undisturbed cumulate, chevron, and cornet halite inclusions may retain atmospheric gas during crystallization from shallow saline, lagoonal, and/or saltpan brine. These are the first measurements of inclusion gas for the Neoproterozoic obtained from 815 ± 15–m.y.–old Browne Formation chevron halite of the Officer Basin, southwest Australia. The 31 gas measurements afford us a direct glimpse of the composition of the mid- to late Neoproterozoic atmosphere and register an average oxygen content of 10.9%. The measured pO_2 puts oxygenation of Earth's paleoatmosphere ~100–200 m.y. ahead of current models and proxy studies. It also puts oxygenation of the Neoproterozoic atmosphere in agreement with time of diversification of eukaryotes and in advance of the emergence of marine animal life.

INTRODUCTION

Deciphering the oxygenation history of the atmosphere and oceans is critical to understanding weathering processes, sedimentary environments, climate change, mass extinctions, tectonic events, and the evolution of Earth's biota. Earth's atmosphere was not always plentiful in free oxygen, and finding a paleobarometer to measure its partial pressure over geologic time remains "a famously difficult challenge" (Lyons et al., 2014, p. 307). Accurately defining Archean, Proterozoic, as well as Phanerozoic atmospheric conditions remains problematic, despite the multitude of proxies from marine and non-marine archives (metals and isotopes of U, Cr, Mo, S, Zn, Fe, Se, C) for modeling atmospheric conditions (Lyons et al., 2014; Kunzmann et al., 2015; Liu et al., 2015; Sperling et al., 2015). Indeed, according to Canfield (2005, p. 1), the "sparse geologic record combined with [geochemical] uncertainties...yields only a fragmentary and imprecise reading of atmospheric oxygen evolution." Major steps in unraveling the evolution of atmospheric oxygen and its close link to the evolution of life on Earth have produced some revolutionary hypotheses and concepts. In 1998, Canfield suggested that the deep ocean of the mid-Proterozoic was anoxic and ferruginous and atmospheric oxygen was <0.1% (Canfield, 1998). However, much remains to be quantified about the redox state of the Proterozoic ocean and atmosphere (Lasaga and Ohmoto, 2002; Canfield, 2005) and especially the emergence of marine animal life during the Neoproterozoic (Canfield et al., 2007; Lyons et al., 2014).

The increasing number of elemental and isotopic proxies give us a better understanding of the "relative" redox state of the atmosphere and ocean during Earth's early history, which shows that most of it was marked by low oxygen levels with two exceptional perturbations termed the Great Oxidation Event (GOE) and Neoproterozoic Oxidation Event (NOE). The models of earliest oxygen evolution document the GOE but are quite uncertain about the NOE (magnitude, onset, and trend) and its relationship to the diversification of plant life and the evolution of marine animal life. Several models suggest persistence of extremely low oxygen levels for this time period (Lyons et al., 2014), whereas others advocate more moderate and increasing but uncertain levels (Canfield, 2005, his figure 6). Most of these models leave unresolved the question of whether oxygenation of the atmosphere-ocean drove animal evolution or animal evolution drove oxygenation (Lyons et al., 2014).

Halite is well established as a paleoenvironmental archive through analysis of fluid trapped in inclusions (Benison and Goldstein, 1999). This archive with primary fluid in inclusions is now accepted to stretch back to the Neoproterozoic (Spear et al., 2014). Inclusions in halite may contain two phases consisting of primary evaporative brine and a gas bubble. The gas may reflect the ambient atmosphere, gas trapped in soil/sediment columns, or gas incorporated during diagenesis (Lowenstein and Hardie, 1985; Hovorka, 1987; Schreiber and El Tabakh, 2000). It is our intent to demonstrate that trapped gas in halite is primary and then measure the inclusion gas to document the actual oxygen level of the Neoproterozoic atmosphere (Brand et al., 2015; Blamey et al., 2015).

PRESERVATION CRITERIA

Geologic archives, irrespective of material, whether used for proxy investigation or direct measurements need to be intensively screened for their preservation state (Brand et al., 2011), including our material of choice in this study, halite. We present a number of features and parameters that halite must possess to be considered a robust archive for retaining primary gas contents. Halite from highly concentrated brine (~10.6 seawater enrichment; McCaffrey et al., 1987) starts by forming cumulate crystals at the brine-air interface as floating individuals or rafts (Hovorka, 1987). These crystals will include bands of inclusions acquired during rapid growth, but they eventually settle out to the bottom of salinas, playas, or sabkhas of shallow water depth. Intermittently wet, syntaxial precipitation of halite initiates the formation of chevron and/or cornet crystals (Lowenstein and Hardie, 1985). Chevron halite forms rapidly on the cumulate substrate at the air-brine interface as vertically oriented and elongated crystals with fluid inclusion–rich and milky chevron bands aligned parallel to the crystal faces. With faster

growth, more square to rectangular inclusions may form along the crystal faces, and upward-pointed cubes in continuous and extensive beds form (Schreiber and El Tabakh, 2000). Another type of halite that forms on the cumulate substrate at the air-brine interface are cornet crystals with increasingly widening upward-oriented inclusion bands (Hovorka, 1987). The inclusion bands tend to be parallel to the crystal face and more abundant during rapid daytime growth. In addition, patches of clear halite may be associated with chevron and cornet halite during primary growth but with the exclusion of inclusions (Lowenstein and Hardie, 1985). Halite may also form at subaqueous depth producing few to no inclusions from stratified dysoxic-anoxic bottom water (Schreiber and El Tabakh, 2000).

Overall, the original halite crystal fabric must be devoid of any depositional and/or post-depositional tectonic and/or halotectonic folding, faulting, and fracturing to allow the preservation of bedding and crystal fabrics and textures (Spear et al., 2014). Recrystallized or diagenetically formed halite may be identified by unusually large, distorted, sporadically distributed interlocking mosaics of clear crystals with large and abundant inclusions (Schreiber and El Tabakh, 2000). Halite cement forms during early burial, and the entire process is complete by ~45 m depth (Casas and Lowenstein, 1989), and afterward halite is no longer susceptible to dissolution and alteration except under high-temperature, fluid burial, and tectonic conditions.

Geochemistry may be an additional screening tool to identify the primary state of inclusions in halite. Bromine and $\delta^{34}S$ are two such tools to ascertain the primary and marine nature of halite. The sulfur isotope composition is largely controlled by the sulfur content of the ambient but geologically variable seawater, whereas Br content will range from 65 to 75 ppm at the onset of halite crystallization, depending on the partition coefficient, and reach ~270 ppm at the offset (McCaffrey et al., 1986). Also, the major ion chemistry of the inclusion fluids reflects the preservation potential of the halite (Spear et al., 2014). Maturation of halite deposits is generally complete within 45 m of burial manifested by the occlusion of all intercrystalline porosity by clear halite cement (Schléder et al., 2008).

Halite fluid inclusions may contain oxygenic photoautotrophs such as *Dunaliella* and halophilic Archaea (Schubert et al., 2010), with the former potentially increasing the local oxygen concentration. Halite forms in brines with >325 gL^{-1} salinity that may be replete with halophilic bacteria imparting a red color on the water but lack live oxygenic photoautotrophs, thus local post-depositional oxygen production within inclusions is not an issue. In summary, if depositional conditions and fabric/textural and geochemical parameters support a primary state, then gases trapped in inclusions of cumulate, chevron, and cornet halite may contain gas reflective of the ambient atmosphere at the time of crystallization.

ANALYTICAL METHOD

Halite was cleaned with isopropanol to remove surface organics and air dried, and then placed under vacuum overnight to remove interstitial and intercrystalline gas. A sample consisted of several match head–sized halite pieces (2–4 mm in diameter) that were crushed incrementally to produce five to 12 successive gas bursts. Data acquisition was performed with two Pfeiffer Prisma quadrupole mass spectrometers operating in crush-fast scan (CFS) peak-hopping mode (Parry and Blamey, 2010; Blamey et al., 2015). The instrument was calibrated using Scott Gas Mini-Mix gas mixtures (with 2% uncertainty), and verified with capillary tubes (with 1% uncertainty) filled with gas mixtures, and three in-house fluid inclusion gas standards. Amount of gas was calculated by matrix multiplication to provide quantitative results. Volatiles are reported in mole percent, and the 3σ detection limit for gases is ~0.3 ppm (~1 × 10^{-15} mol; Norman and Blamey, 2001). Precision and accuracy, respectively, of seven capillary tubes with encapsulated atmosphere, in relative percent, were: N_2, 1.43 and 0.05; O_2, 5.13 and 0.05; and Ar, 6.86 and 4.60. The gas results of the capillary tubes cluster close to the global atmospheric gas content (Fig. 1), and they clearly demonstrate the robustness of the CFS-MS method for measuring gas in artificial and natural inclusions. All results of laboratory tubes and modern (Carlsbad [New Mexico, USA], Lake Polaris [Australia]), Messinian, Cretaceous, and Neoproterozoic halite samples are presented as water-free and large gas bursts–free data (see the GSA Data Repository[1]). Some halites produce steady gas burst trends (Carlsbad, Lake Polaris, Messinian, Neoproterozoic 1478 and 1502) that support their homogenous nature and constant environment of crystallization, whereas those with some variability (Cretaceous and remainder Neoproterozoic; Fig. DR1 in the Data Repository) reflect some unknown influences that require more study. However at this time, we overcome that issue by using only averages in our evaluations (Fig. 1).

LIMITATIONS

Obtaining well-preserved halite with abundant gas inclusions despite intensive screening is a challenge. The need for only small inclusions may be a benefit in that areas with cumulate, chevron, or cornet features may be exhumed from large halite crystals for gas analysis. However, small inclusion size and corresponding low gas volumes may hinder their 100% extraction,

[1]GSA Data Repository item 2016211, supplementary figures and analyses, is available online at www.geosociety.org/pubs/ft2016.htm, or on request from editing@geosociety.org.

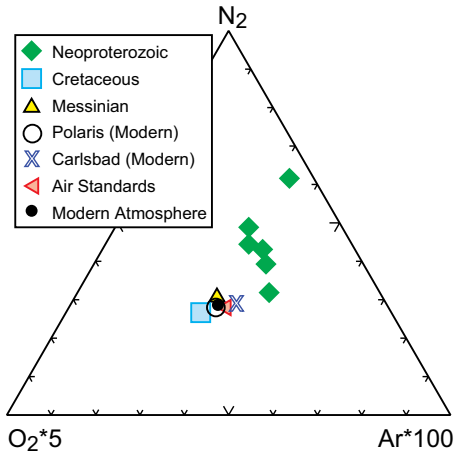

Figure 1. Ternary (N_2-Ar-O_2) diagram of inclusion gases from laboratory capillary tubes (air standards) and of modern and ancient halite compared to modern atmospheric contents. Contents are based on averages for each sample (see the Data Repository [see footnote 1])

and indeed oxygen extracted from one modern cumulate halite (Carlsbad) relative to atmospheric composition is lower by ~9.2%. More study is warranted to evaluate this observation and its potential impact on ancient halite–based oxygen measurements.

METHOD EVALUATION

The initial consideration is the testing of gases obtained from inclusions of modern and ancient cumulate, chevron, and cornet halite to verify the robustness of the archive.

Modern Halite

Modern halite for testing the oxygen paleobarometer were recovered from ponds at the Mosaic salt mine near Carlsbad, New Mexico (USA), and Lake Polaris, Southern Cross (Australia). The material consisted of rafts of cumulate halite growing at the water-atmosphere interface of the ponds, and their inclusions were tested for N_2, O_2, and Ar gas contents. The results fall within acceptable parameters of modern atmospheric air (Fig. 1).

Messinian Halite

Material from the latest Miocene was obtained from the Racalmuto mine of Sicily. Based on its fabric and texture, the halite is of the cornet variety with bands rich in inclusions and precipitated at the water-atmosphere interface (Fig. DR2). Its gas content overlaps significantly with those of the air standards (capillary tubes) and modern halite from Carlsbad (Fig. 1). This suggests little change in atmospheric oxygen over the past 6 m.y.

Cretaceous Halite

Material from this period covers a time of controversial atmospheric oxygen gas contents (Berner and Landis, 1988; see Fig. DR3). Chevron halite from the Cretaceous Mengyejing

Formation of Tibet gives average oxygen of 25.8%, which is higher than the modern level of 20.946% (Fig. 1), and supports the assertion of elevated pO_2 during the mid-Cretaceous. It is highly unlikely that oxygen could have been injected into halite inclusions without evidence of morphochemical disruption, and we must conclude that Cretaceous atmospheric oxygen was most likely higher than present-day levels. The tests performed on the modern, Messinian, and Cretaceous halites support halite's robustness as an atmospheric oxygen archive.

NEOPROTEROZOIC HALITE AND ATMOSPHERE

Our Neoproterozoic halite samples are from the Empress 1A and Lancer 1 drill cores from the Officer Basin, southwestern Australia (Fig. 2), a broad marine shelf tectonically stable since Neoproterozoic time (Figs. DR4 and DR5). The samples at the two localities are from the "B" interval of the Browne Formation (Fig. DR6) that is bracketed to 830–800 Ma based on chemostratigraphy and geochronology (Hill and Walter, 2000; Swanson-Hysell et al., 2015). In summary, the halite samples were screened for their preservation using petrography, chemistry, and stable isotope compositions (Lécuyer and O'Neil, 1994; Spear et al., 2014), and Table 1 summarizes the fabric and geochemical parameters.

The Neoproterozoic halite inclusion gases are all oxygen depleted relative to modern atmosphere (Fig. 1; Fig. DR1). Inclusion oxygen from sample 1478 (Empress core) is low at 1.64%, and based on depositional and geochemical features, the halite formed in the salt basin during rising water level and in dysoxic bottom water (Schreiber and El Tabakh, 2000). In contrast, the other halite samples from the Neoproterozoic Browne Formation are replete with bands rich in fluid/gas inclusions (Fig. 3). CFS-MS analysis of inclusions shows average oxygen contents ranging from 10.15% to 13.43% (Table 1). Thus, atmospheric oxygen during the mid-Neoproterozoic was on average 10.9% or about half of the modern level of 20.95%.

TABLE 1. GEOCHEMISTRY OF HALITE (Br, $\delta^{34}S$) AND EXTRACTED FLUIDS (Na^+, Ca^{2+}, Mg^{2+}, Cl^-) AND OXYGEN GAS CONTENT OF NEOPROTEROZOIC BROWNE FORMATION HALITE, OFFICER BASIN, AUSTRALIA, AND MODELED GEOCHEMISTRY OF NEOPROTEROZOIC SEAWATER, MODERN SEAWATER, AND ATMOSPHERE

Depth (m)	Texture	Br (ppm)	$\delta^{34}S$ (‰)	Na^+	Ca^{2+}	Mg^{2+}	Cl^-	pO_2 at 1 bar (%)
				(mMol/kg H_2O)				
E1478*	Chevron	–	–	592	388	3550	8466	1.64
E1479	Chevron	73	15.2	–	–	–	–	–
E1482	Chevron	–	–	290	553	4283	9828	10.48
E1484.5	Chevron	91	15.3	–	–	–	–	–
E1492	Chevron	93	15.4	555	393	3440	8345	10.21
E1496	Chevron	103	15.5	–	–	–	–	–
E1497	Chevron	–	–	598	423	3498	8473	10.15
L1466.3		–	–	470	508	3924	9348	10.23
L1465.5		107	15.1	–	–	–	–	–
E1502	Chevron	122	15.3	–	–	–	–	–
E1502.2	Chevron	–	–	506	323	3741	8651	13.43
Neo-SW†	–	–	17.0[1]	456	11	48	565	10.90
SW[2]	65 (75)–270[3]		21.0	485	11	55	565	20.95

*E—Empress drill hole; L—Lancer drill hole.
Note: Halite texture, cf. Lowenstein and Hardie (1985). Neo-SW—Neoproterozoic seawater; SW—modern seawater; dash is No Data. References: 1—Canfield (2005); 2—Lowenstein et al. (2005); 3—Schreiber and El Tabakh (2000).
†Geochemistry from Spear et al. (2014).

DISCUSSION

Gas analysis in halite has evolved from methods requiring large samples with large inclusions of low resolution to methods using heat or cold extraction (CFS) and measuring by mass spectrometry requiring smaller samples with smaller inclusions of much higher resolution (Blamey, 2012).

Three models of atmosphere and ocean oxygenation place onset of the NOE somewhere between 500 (Sperling et al., 2015) and 800 Ma (Liu et al., 2015). The first model is essentially unidirectional with two major step increases in both atmospheric and oceanic oxygen (red band, Fig. 4), the second model offers up a more gradual and uncertain increase during the mid-Neoproterozoic (blue band, Fig. 4), and the third model espoused by Canfield (2005, his figure 6) expresses a greater degree of uncertainty during Neoproterozoic oxygenation (dashed line with question marks in Fig. 4). Our measured average atmospheric oxygen of 10.9% is well above levels of all major models (Fig. 4). The atmospheric oxygen contents and commensurate levels in seawater proposed by the models are too low to sustain the emergence of animal life (Knoll, 1992), and the increases in oxygen postulated for the late Cryogenian and mid-Ediacaran are too late to trigger the emergence of marine life (Sperling et al., 2015). Instead, our measured level of oxygen for the mid- to late Tonian (Neoproterozoic) atmosphere is more than sufficient to support the expansion of plant life and facilitate the emergence of marine animals. Furthermore, our atmospheric oxygen measurements infer that the NOE took place at least 200–100 m.y. prior to that suggested by most models based on proxies.

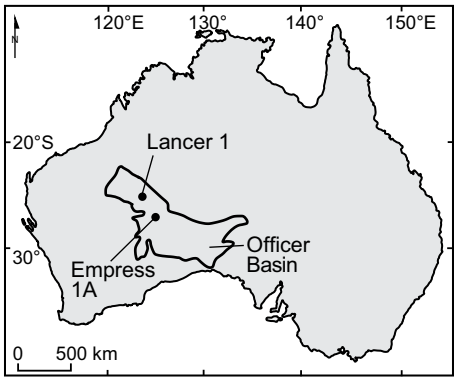

Figure 2. Setting of Officer Basin in southwestern Australia showing locations of Lancer 1 and Empress 1A drill cores and sampling horizons in Browne Formation (modified from Spear et al., 2014).

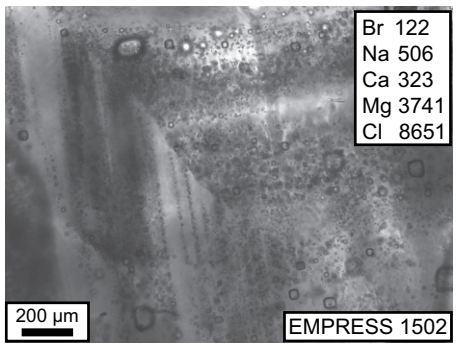

Figure 3. Thin section view of halite sample 1502 from the Empress 1A core (Officer Basin, Australia). Undisturbed chevron bands with gas/fluid inclusions are clearly visible in photograph (modified from Spear et al., 2014). Upward crystal growth is in direction of chevron tip (upper left corner), and geochemical concentrations (e.g., Br) are in parts per million.

CONCLUSIONS

We provide the first direct measurements of the oxygen content of the Neoproterozoic atmosphere. After extensive and careful screening of ancient halite crystals, our analysis of Neoproterozoic halite inclusions and their gases sealed during crystallization confirms that average oxygen levels ~815 m.y. ago were 10.9%. Our atmospheric oxygen measurements indicate an oxygenated environment in which complex life could have emerged and flourished in advance

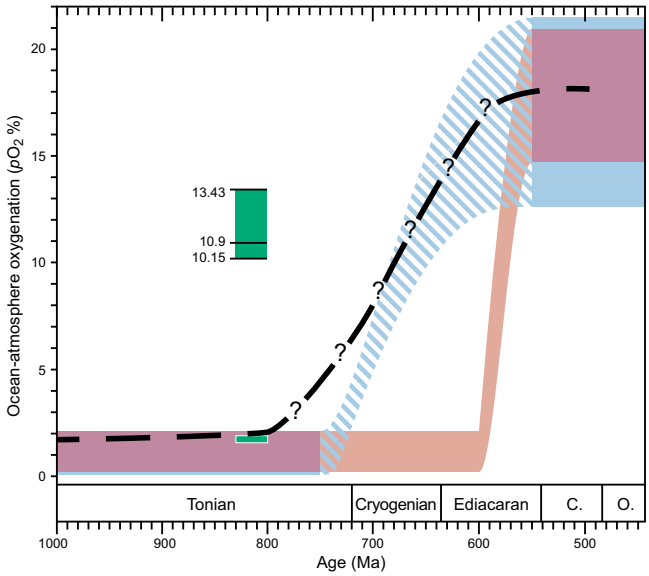

Figure 4. Atmosphere and ocean oxygenation trends during Neoproterozoic. Dashed line is proposed atmospheric oxygen trend by Canfield (2005), red unidirectional curve represents traditional viewpoint (e.g., Kump, 2008), and blue curve represents emerging model presented by Lyons et al. (2014). Green field shows our atmospheric oxygen measurements for Tonian time during Neoproterozoic (Table 1). C.—Cambrian; O.—Ordovician.

of the Ediacaran and Cambrian explosions. Our direct analysis of gas-bearing inclusions in halite places atmospheric and shallow ocean oxygenation ~100–200 m.y. in advance of most proxy-based models. Inclusion gas analysis of primary halite is a new and novel paleobarometer of atmospheric oxygen with many potential terrestrial and extraterrestrial applications.

ACKNOWLEDGMENTS

We thank the Geological Survey of Australia for permission to sample the Empress 1A and Lancer 1 cores, the Natural Sciences and Engineering Research Council of Canada for financial support (grant #7961–15) of U. Brand, and the National Natural Science Foundation of China for support of F. Meng and P. Ni (grants 41473039 and 4151101015). We thank M. Lozon (Brock University) for drafting and constructing the figures. We thank the editor, Brendan Murphy, as well as three reviewers (Steve Kesler, Erik Sperling, and an anonymous reviewer), for improving the manuscript into its final form.

REFERENCES CITED

Benison, K.C., and Goldstein, R.H., 1999, Permian paleoclimate data from fluid inclusions in halite: Chemical Geology, v. 154, p. 113–132, doi:10.1016/S0009-2541(98)00127-2.

Berner, R.A., and Landis, G.P., 1988, Gas bubbles in fossil amber as possible indicators of the major gas composition of ancient air: Science, v. 239, p. 1406–1409, doi:10.1126/science.239.4846.1406.

Blamey, N.J.F., 2012, Composition and evolution of crustal, geothermal and hydrothermal fluids interpreted using quantitative fluid inclusion gas analysis: Journal of Geochemical Exploration, v. 116–117, p. 17–27, doi:10.1016/j.gexplo.2012.03.001.

Blamey, N.J.F., Parnell, J., McMahon, S.M., Mark, D.F., Tomkinson, T., Lee, M., Shivak, J., Izawa, M.R.M., Banerjee, N.R., and Flemming, R.L., 2015, Evidence for methane in Martian meteorites: Nature Communications, v. 6, 7399, doi:10.1038/ncomms8399.

Brand, U., Logan, A., Bitner, M.A., Griesshaber, E., Azmy, K., and Buhl, D., 2011, What is the ideal proxy of Palaeozoic seawater chemistry?: Memoirs of the Association of Australasian Palaeontologists, v. 41, p. 9–24.

Brand, U., Blamey, N.J.F., Spear, N., Parnell, J., and MacMahon, S., 2015, Neoproterozoic atmospheric oxygen and the diversification of metazoan and animal life, *in* Proceedings, 25th Goldschmidt Conference, Prague, Czech Republic, 16–21 August: Cambridge, UK, Cambridge Publications Ltd., Session 22c, p. 375.

Canfield, D.E., 1998, A new model for Proterozoic ocean chemistry: Nature, v. 396, p. 450–453, doi:10.1038/24839.

Canfield, D.E., 2005, The early history of atmospheric oxygen: Homage to Robert M. Garrels: Annual Reviews of Earth and Planetary Science, v. 33, p. 1–36, doi:10.1146/annurev.earth.33.092203.122711.

Canfield, D.E., Poulton, S.W., and Narbonne, G.M., 2007, Late-Neoproterozoic deep-ocean oxygenation and the rise of animal life: Science, v. 315, p. 92–95, doi:10.1126/science.1135013.

Casas, E., and Lowenstein, T.K., 1989, Diagenesis of saline pan halite: Comparison of petrographic features of modern, Quaternary and Permian halites: Journal of Sedimentary Petrology, v. 59, p. 724–739.

Hill, A.C., and Walter, M.R., 2000, Mid-Proterozoic (~830–750 Ma) isotope stratigraphy of Australia and global correlation: Precambrian Research, v. 100, p. 181–211, doi:10.1016/S0301-9268(99)00074-1.

Hovorka, S., 1987, Depositional environments of marine-dominated bedded halite, Permian San Andres Formation, Texas: Sedimentology, v. 34, p. 1029–1054, doi:10.1111/j.1365-3091.1987.tb00591.x.

Knoll, A.H., 1992, The early evolution of eukaryotes: A geological perspective: Science, v. 256, p. 622–627, doi:10.1126/science.1585174.

Kump, L.R., 2008, The rise of atmospheric oxygen: Nature, v. 451, p. 277–278, doi:10.1038/nature06587.

Kunzmann, M., Halverson, G.P., Scott, C., Minarik, W.G., and Wing, B.A., 2015, Geochemistry of Neoproterozoic black shales from Svalbard: Implications for oceanic redox conditions spanning Cryogenian glaciations: Chemical Geology, v. 417, p. 383–393, doi:10.1016/j.chemgeo.2015.10.022.

Lasaga, A.C., and Ohmoto, H., 2002, The oxygen geochemical cycle: Dynamics and stability: Geochimica et Cosmochimica Acta, v. 66, p. 361–381, doi:10.1016/S0016-7037(01)00685-8.

Lécuyer, C., and O'Neil, J.R., 1994, Stable isotope compositions of fluid inclusions in biogenic carbonates: Geochimica et Cosmochimica Acta, v. 58, p. 353–363, doi:10.1016/0016-7037(94)90469-3.

Liu, X., Kah, L.C., Knoll, A.H., Cui, H., Kaufman, A.J., Shahar, A., and Hazen, R.M., 2015, Tracing Earth's O_2 evolution using Zn/Fe ratios in marine carbonates: Geochemical Perspectives, v. 2, p. 24–34, doi:10.7185/geochemlet.1603.

Lowenstein, T.K., and Hardie, L.A., 1985, Criteria for the recognition of salt-pan evaporates: Sedimentology, v. 32, p. 627–644, doi:10.1111/j.1365-3091.1985.tb00478.x.

Lowenstein, T.K., Timofeeff, M.N., Kovalevych, V.M., and Horita, J., 2005, The major-ion composition of Permian seawater: Geochimica et Cosmochimica Acta, v. 69, p. 1701–1719, doi:10.1016/j.gca.2004.09.015.

Lyons, T.W., Reinhard, C.T., and Planavsky, N.J., 2014, The rise of oxygen in Earth's early ocean and atmosphere: Nature, v. 506, p. 307–315, doi:10.1038/nature13068.

McCaffrey, M.A., Lazar, B., and Holland, H.D., 1987, The evaporation path of seawater and the coprecipitation of Br^- and K^+ with halite: Journal of Sedimentary Petrology, v. 57, p. 928–937.

Norman, D.I., and Blamey, N.J.F., 2001, Quantitative gas analysis of fluid inclusion volatiles by a two quadrupole mass spectrometer system, *in* Proceedings, European Current Research On Fluid Inclusions XVI, Porto, Portugal, 02 to 04 May 2001, Abstracts: Porto, Portugal, Universidade do Porto, Departamento de Geologia Faculdade de Ciências, p. 341–344.

Parry, W.T., and Blamey, N.J.F., 2010, Fault fluid composition from fluid inclusion measurements, Laramide age Uinta thrust fault, Utah: Chemical Geology, v. 278, p. 105–119, doi:10.1016/j.chemgeo.2010.09.005.

Schléder, Z., Urai, J.L., Nollet, S., and Hilgers, C., 2008, Solution-precipitation creep and fluid flow in halite: A case study of Zechstein (Z1) rocksalt from Neuhof salt mine (Germany): International Journal of Earth Sciences, v. 97, p. 1045–1056, doi:10.1007/s00531-007-0275-y.

Schreiber, B.C., and El Tabakh, M., 2000, Deposition and early alteration of evaporites: Sedimentology, v. 47, p. 215–238, doi:10.1046/j.1365-3091.2000.00002.x.

Schubert, B.A., Timofeeff, M.N., Lowenstein, T.K., and Polle, J.E.W., 2010, *Dunaliella* cells in fluid inclusions in halite: Significance for long-term survival of prokaryotes: Geomicrobiology Journal, v. 27, p. 61–75, doi:10.1080/01490450903232207.

Spear, N., Holland, H.D., Garcia-Veigas, J., Lowenstein, T.K., Giegengack, R., and Peters, H., 2014, Analyses of fluid inclusions in Neoproterozoic marine halite provide oldest measurement of seawater chemistry: Geology, v. 42, p. 103–106, doi:10.1130/G34913.1.

Sperling, E.A., Wolock, C.J., Morgan, A.S., Gill, B.C., Kunzmann, M., Halverson, G.P., Macdonald, F.A., Knoll, A.H., and Johnston, D.T., 2015, Statistical analysis of iron geochemical data suggests limited late Proterozoic oxygenation: Nature, v. 523, p. 451–454, doi:10.1038/nature14589.

Swanson-Hysell, N.L., Maloof, A.C., Condon, D.J., Jenkin, G.R.T., Alene, M., Tremblay, M.M., Tesema, T., Rooney, A.D., and Haileab, B., 2015, Stratigraphy and geochronology of the Tambien Group, Ethiopia: Evidence for globally synchronous carbon isotope change in the Neoproterozoic: Geology, v. 43, p. 323–326, doi:10.1130/G36347.1.

Manuscript received 28 March 2016
Revised manuscript received 7 June 2016
Manuscript accepted 9 June 2016

Printed in USA